HiSST: 4th International Conference on High-Speed Vehicle Science Technology
22 -26 September 2025, Tours, France

Effect of combustion instability on propagation mode of rotating detonation engine

*Sijia Gao[1, 2, 3], Han Peng[1], Zhipeng Sun[1], Huan Lian[2], Yue Huang[1, *], Zijun Zhou[1] and Yancheng You[1]*

[1]School of Aerospace Engineering, Xiamen University, Xiamen 361005, China
[2]State Key Laboratory of High Tempera Gas Dynamics, Institute of Mechanics, Chinese Academy of Sciences, Beijing 100190, China
[3]School of Engineering Science, University of Chinese Academy of Sciences, Beijing 100190, China
Corresponding author: Yue Huang, huangyue@xmu.edu.cn

Abstract

Rotating detonation waves exhibit different propagation modes under varying operating conditions. Two-dimensional Navier-Stokes equations and a kerosene/air reaction model based on RYrhoCentralFoam solver were used to simulate the non-premixed two-phase rotating detonation combustion. The transformation trends and evolution processes of the propagation modes of the rotating detonation wave were analyzed in response to variations in the total temperature of the incoming flow and in the fuel droplet proportion. Additionally, the vaporization rate of liquid fuel within the flow field was examined, and the third Damköhler number as well as the transient Rayleigh index of the rotating detonation combustion flow were calculated. The results indicate that increasing the total temperature of the incoming flow and decreasing the fuel droplet proportion lead to an increase in the number of detonation waves. Higher incoming flow temperatures correspond to lower peak pressures of the detonation waves, more numerous detonation fronts, and a faster mode transition. Conversely, reducing the total temperature maintains the number of detonation waves but results in increased wave intensity. An elevated vaporization rate of liquid droplets induces a quasi-isovolumetric combustion process within the detonation flow field, generating pressure shocks. The interaction between these pressure shocks and heat release contributes to the overall dynamics. Based on the self-sustaining energy growth characteristic of thermoacoustic instability, the system undergoes multiple cycles of decoupling and re-detonation, ultimately forming a stable detonation wave and leading to a transformation in the propagation mode.

Keywords: *rotating detonation; liquid kerosene; propagation mode; thermoacoustic instability*

1. Introduction

In comparison to traditional isobaric combustion, detonation combustion necessitates a lower increase in entropy to achieve higher pressure [1]. Rotating detonation engines (RDEs) have garnered increasing interest in recent years owing to their advantages, including elevated heat release intensity, uncomplicated structures, and high theoretical thermodynamic cycle efficiency [2-4]. Detonation represents an inherently unsteady combustion phenomenon characterized by the continuous propagation of one or more detonation waves along the annular wall of the combustor. The configuration of detonation waves in terms of their number and propagation direction, referred to as the propagation mode, constitutes a multifaceted issue that presently lacks a definitive understanding concerning its operational dynamics and root causes. Extensive experiments and numerical simulations have been conducted to explore the propagation mode of RDEs.

In previous investigations, detonation waves have been observed to operate in various modes, including stable single wave mode, single wave/multiple waves hybrid mode, stable multiple waves mode, multiple waves collision mode, and longitudinal pulsed detonation [5-7]. Recent researches have highlighted that the propagation mode in RDEs is influenced by a multitude of factors, encompassing the fuel [8-11], mass flow of reactants [6,12,13], equivalence ratio [14-18], injection geometries (injection scheme, shrinkage ratio, injector pressure drop) [19-23], detonation channel geometries [24,25], and nozzles [26,27]. RDEs exhibit the capability to function in diverse propagation modes even with identical mass flow rates, or conversely, to retain a consistent propagation mode amidst fluctuations in mass flow rates [28]. Adding a small amount of ozone to the reactants can enhance the ignition process of RDW, leading to a transition from single wave mode to multiple waves mode, but has no obvious effect on the propulsion performance of RDE [29]. In the context of nozzles, five distinct wave propagation modes can be identified: single wave mode, counter-rotating wave mode, self-adjustive mode, periodic oscillation mode, and deflagration mode. While in the same conditions, only single wave mode is observed with no nozzle [30]. The multiplicity is closely related to the non-uniform distribution of the RDW, and the decrease of the uniformity leads to the increase of the number of the RDWs [22].

Research on RDCs utilizing gas fuels has been extensively conducted, revealing that the choice of fuel significantly influences the propagation modes of RDWs. However, RDWs tend to exhibit distinct propagation modes when using liquid kerosene compared to gas fuels. The application of liquid fuels in RDCs and their associated effects remain largely underexplored, warranting further investigation into the propagation modes associated with liquid fuels. This study aims to address this gap.

In summary, research on the propagation modes of RDWs has been ongoing, focusing on the causes and control methods of mode transitions. However, the complex flow field within RDCs introduces significant uncertainties, and there remains a notable gap in the study of two-phase RDEs. To further investigate the factors influencing propagation modes during the detonation process of liquid kerosene RDEs, a two-dimensional numerical simulation was performed on a non-premixed liquid kerosene/air RDE by solving the compressible two-phase reactive Navier-Stokes equations. The study revealed that the propagation mode of RDWs varies with inflow conditions, and the mechanisms behind these transformations were analyzed in terms of the vaporization rate of fuel droplets. Additionally, methods for regulating the propagation modes of RDWs were explored.

2. Numerical method and calculation model

2.1. Numerical method

The cases in this study are simulated using the RYrhoCentralFoam solver based on OpenFOAM. The compressible Navier-Stokes equations are solved as governing equations and are discretized using the finite volume method. The second-order implicit backward method is employed for temporal discretization with the adaptive time step, which is about 5*10-9 s (Courant number is about 0.1). The convective terms of the momentum equation employ the second-order Godunov central-upwind scheme developed by Kurganov et al. [31] The convective terms of the energy and component mass fraction equation employ the total variation diminishing (TVD) scheme. The diffusion terms adopt the second-order central difference scheme. In recent years, the RYrhoCentralFoam solver has been successfully applied to the simulations of RDE in gas and liquid phases [32-34]. In this study, a simplified 6-species-2-step mechanism for kerosene/air is used for the chemical reaction.

The liquid phase governing equations are solved using a first-order implicit Euler method, while the gas properties near the droplets are computed via linear interpolation. At each time step, a two-way coupling accounts for the exchange of mass, momentum, and energy between the gas and liquid phases.

2.2. Calculation model

The physical model used for numerical simulation in this study is shown in Fig. 1. The computational domain is a two-dimensional rectangular domain with a length of 300 mm and a width of 185 mm. The channel width is relatively small compared with the diameter of the annular RDE. As a result, the annular RDE can be expanded into the two-dimensional domain by ignoring the three-dimensional effects to reduce the computational cost.

The boundary conditions are also marked in Fig. 1. The left and right boundaries are periodic to simulate a continuous RDC. The bottom boundary is the air inlet boundary. The air is injected into the chamber through a series of micro nozzles located 75 mm from the inlet boundary. The width of nozzle exit is 6 mm and the width of nozzle throat is 2 mm. The gaseous kerosene fuel is injected through fifty slits of 0.4 mm from the side of the nozzle throat. The mass flow inlet boundary conditions are adopted to the air and kerosene inlet and the global equivalence ratio is stoichiometric ratio. The ignition region is set to 50 MPa and 3000 K of air mixed with kerosene in stoichiometric ratio with a length of 110 mm and a width of 2 mm. The premixed region is set to 0.4 MPa and 300 K of air mixed with kerosene in stoichiometric ratio with a length of 198 mm and a width of 10 mm. The remaining initial region is set to 0.1 MPa and 300 K of air. The ignition region and the premixed region are specified to ignite the detonation wave and stabilize it rapidly in a specified direction. The top boundary is the outlet boundary which is open to the atmosphere of 0.1 MPa and 300 K.

The reaction of kerosene and air is selected as a two-step chemical reaction model [35] considering the computational costs. The kerosene is referred as $C_{10}H_{22}$. The chemical reaction mode contains six species ($C_{10}H_{22}$, O_2, CO, CO_2, H_2O, N_2) and is composed of three reactions corresponding to the fuel oxidation into CO and H_2O, and CO-CO_2 equilibrium [36].

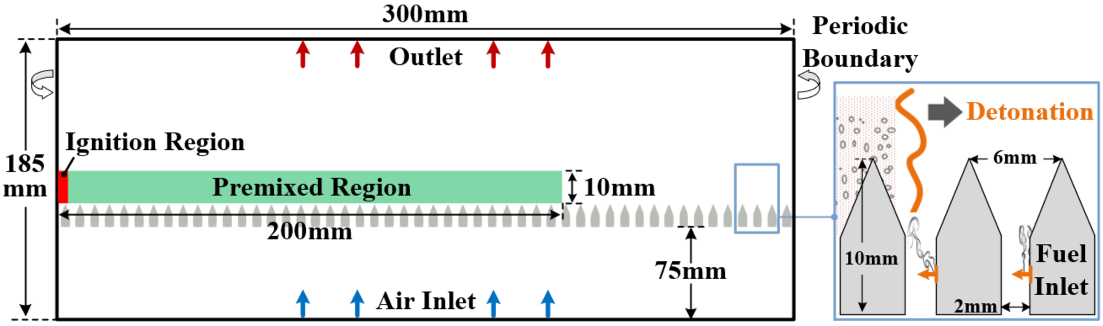

Fig 1. Schematic of the computational domain and boundary conditions

2.3. Mesh independence study

To test the accuracy of the numerical simulations, three scales of meshes are studied with the same computational set-ups. The coarse, medium and fine mesh have a mesh size of 0.25 mm × 0.25 mm, 0.2 mm × 0.2 mm and 0.1 mm × 0.1 mm, respectively. The pressure profiles are used to compare the numerical results with the different meshes. Figure 2 shows that these three meshes present the same location of detonation front and the close peak pressure. The medium mesh provides a closer result with the fine mesh in terms of the post-detonation pressure. Considering the balance of the computational cost and accuracy, the medium mesh is used for the following cases in this study.

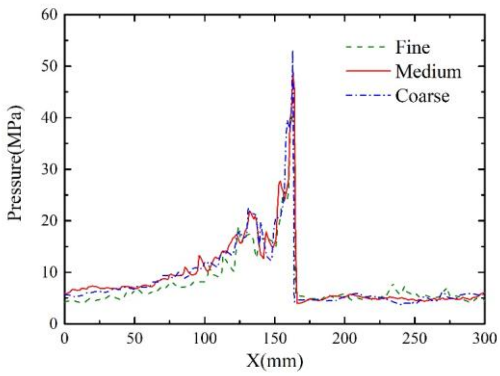

Fig 2. Comparison of pressure profiles on three meshes

3. Results and discussion

3.1. Effect of incoming flow temperature on propagation mode

Previous studies have shown that the incoming flow temperature significantly influences the propagation mode, with mode transitions occurring as the temperature varies. In this study, when the detonation wave is operating stably, the incoming flow temperature is instantaneously increased or decreased to investigate the transformation behavior of the propagation mode. Table 1 presents the inlet flow conditions used in the numerical simulations for this section. The air mass flow rate is 2 kg/s, and the total kerosene mass flow rate is 0.1334 kg/s.

Table 1. Numerical conditions

	T_0 (K)	Droplet volume fraction	Propagation mode
Case 1	600	0.01%	Single wave
Case 2	600 to 700	0.01%	Double waves
Case 3	600 to 800	0.01%	Triple waves
Case 4	700 to 600	0.01%	Double waves
Case 5	800 to 600	0.01%	Triple waves

Figure 3 illustrates the RDW flow fields for Cases 1 to 5. In Case 1, a stable single wave mode is established, exhibiting characteristic RDW flow structures such as the detonation wave, oblique shock wave, reactant filling region, and contact surface. Slight deflagration occurs at the contact surface, while the reactant filling region maintains a stable triangular shape.

When the single wave mode of Case 1 is stable, Cases 2 and 3 are obtained by increasing the incoming flow temperature. In Case 2, the incoming flow temperature rises from 600 K to 700 K, resulting in a transformation of the propagation mode from single wave to co-directional double waves. This change leads to a decrease in detonation wave intensity, a more disordered flow field structure, and an increase in deflagration phenomena within the reactant filling region. In Case 3, the incoming flow temperature is further increased from 600 K to 800 K, causing the propagation mode to shift from single wave to co-directional triple waves. Compared to Case 2, the intensity of the RDWs is further diminished, and the flow field structure becomes even more chaotic. The reactant filling region is nearly completely pre-burned, with the structures of the detonation waves and oblique shock waves becoming indistinct, indicating that the flow field is no longer sufficiently stable. This demonstrates that while increasing the incoming flow temperature can increase the number of RDWs and reduce their intensity. Furthermore, variations in incoming flow temperature significantly influence the number of RDWs generated.

Building on the stable detonation waves observed in Cases 2 and 3, the incoming flow temperature is decreased back to 600 K in Cases 4 and 5, ultimately resulting in stable RDWs. In Case 4, the incoming flow temperature is lowered from 700 K to 600 K, and while the number of RDWs remains unchanged, still exhibiting a double wave configuration, the flow field structure becomes clearer and more stable, with a reduction in the pre-burned phenomenon, even less than that observed in Case 1. In Case 5, the incoming flow temperature is decreased from 800 K to 600 K, and the variation trend of the flow field mirrors that of Case 4. This indicates that the number of RDWs does not decrease with the reduction in incoming flow temperature.

The final incoming flow conditions for Cases 1, 4, and 5 are the same, yet the number of detonation waves differs, indicating that the primary factor influencing the propagation mode of the detonation waves is the "change process" associated with the increase in incoming flow temperature. As the temperature of the incoming flow rises, new hotspots are created within the detonation flow field, leading to the formation of a second or even a third detonation wave. When the incoming flow conditions are sufficient to sustain the current detonation wave mode, reducing the incoming flow temperature does not affect the number of detonation waves, thereby allowing for effective control of the detonation wave propagation mode.

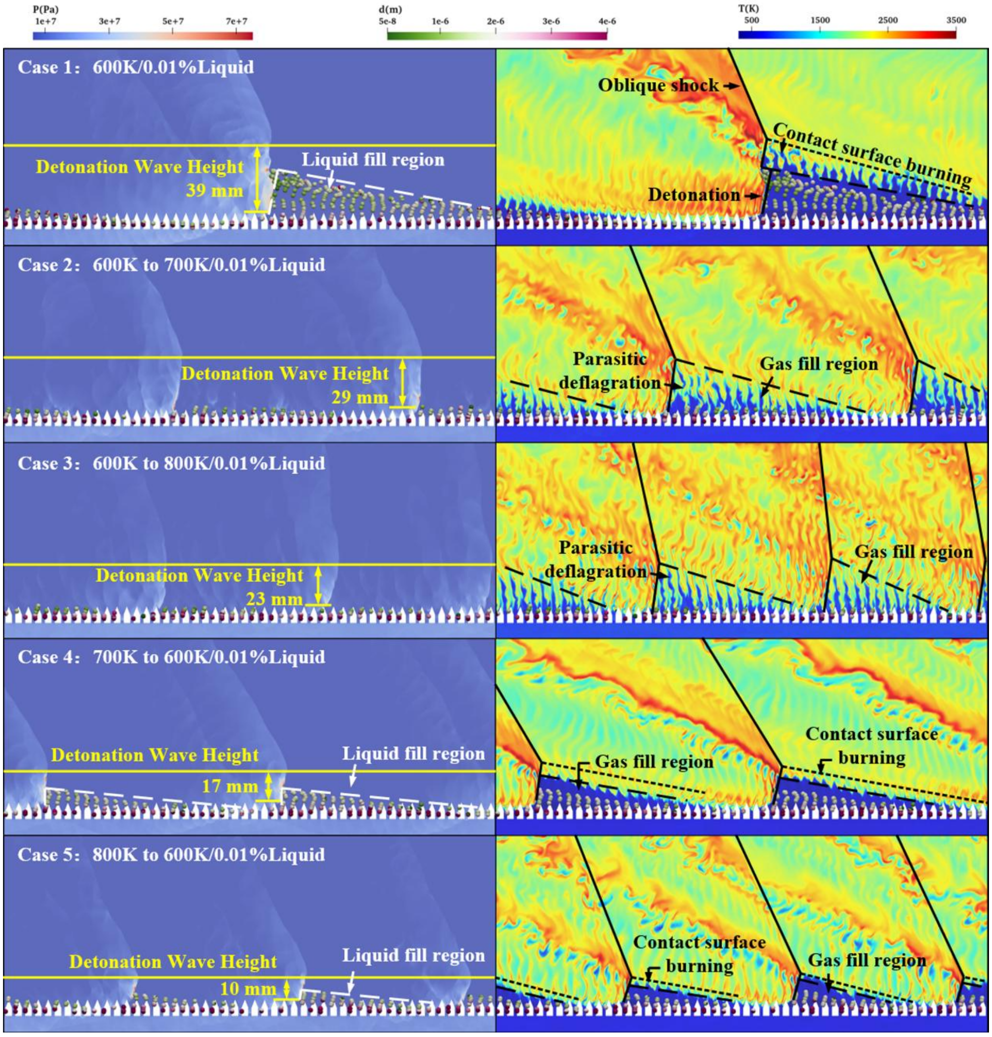

Fig 3. Instantaneous temperature and pressure for Cases 1 to 5

3.2. Effect of liquid kerosene volume fraction on propagation mode

According to the study in Section 3.1, the number of RDWs increases with an increase in incoming flow temperature but does not decrease with a decrease in incoming flow temperature. This suggests that while the incoming flow temperature influences the transformation of the propagation mode, the relationship is not a simple linear one. The incoming flow temperature is merely a surface phenomenon, and the fundamental reason lies in the change in the vaporization rate of the droplets resulting from variations in the incoming flow temperature. This section examines how the propagation mode varies with a decrease in the liquid fraction in the two-phase rotating detonation. Table 2 presents the incoming flow conditions for the numerical simulations of rotating detonation discussed in this section, with an air mass flow rate of 2 kg/s and a total kerosene mass flow rate of 0.1334 kg/s.

Table 2. Numerical conditions

	T_0 (K)	Droplet volume fraction	Propagation mode
Case 6	600	0.01% to 0.001%	Double waves
Case 7	600	0.01% to 0	Double waves
Case 8	700	0.01% to 0.001%	Double waves
Case 9	800	0.01% to 0.001%	Triple waves
Case 10	(700 to) 600	0.01% to 0.001%	Double waves

Figure 4 illustrates the RDW flow fields in Cases 6 to 10. Case 6 is derived by modifying the flow conditions of the stabilized Case 1. Specifically, the volume fraction of kerosene droplets decreases from 0.01% to 0.001%, resulting in a significant reduction in the number of kerosene droplets within the flow field. Consequently, the number of detonation waves increases, and the mode shifts from a single wave to double waves. Additionally, the combustion intensity at the contact surface decreases. In Case 7, the volume fraction of kerosene droplets decreases further from 0.01% to 0, representing a gaseous rotating detonation combustor. The detonation wave propagation mode also transitions from a single wave to double waves, and the height of the detonation wave decreases, consistent with the trend observed in Section 3.1. However, the combustion at the contact surface is more intense than in Case 6, and the temperature within the flow field is higher.

Cases 8 to 10 are obtained by varying the inflow conditions from the stabilized Cases 2 to 4. The volume fraction of kerosene droplets decreases from 0.01% to 0.001%, but the number of detonation waves remains consistent with the previous case. Since the incoming flow temperatures for Cases 2 and 3 are 700 K and 800 K, respectively, the kerosene droplets in the combustion chamber evaporate rapidly, resulting in a very low number of kerosene droplets in the flow field. Consequently, the reduction in the volume fraction of kerosene droplets does not significantly affect the evaporation dynamics of the droplets in the flow field. Compared to Case 4, although the number of kerosene droplets in the flow field of Case 10 has decreased, the detonation wave mode remains unchanged. This suggests that the changes in the detonation wave mode cannot be determined only by the number of droplets in the flow field. Instead, a more detailed analysis of parameters such as the vaporization rate of the droplets is necessary.

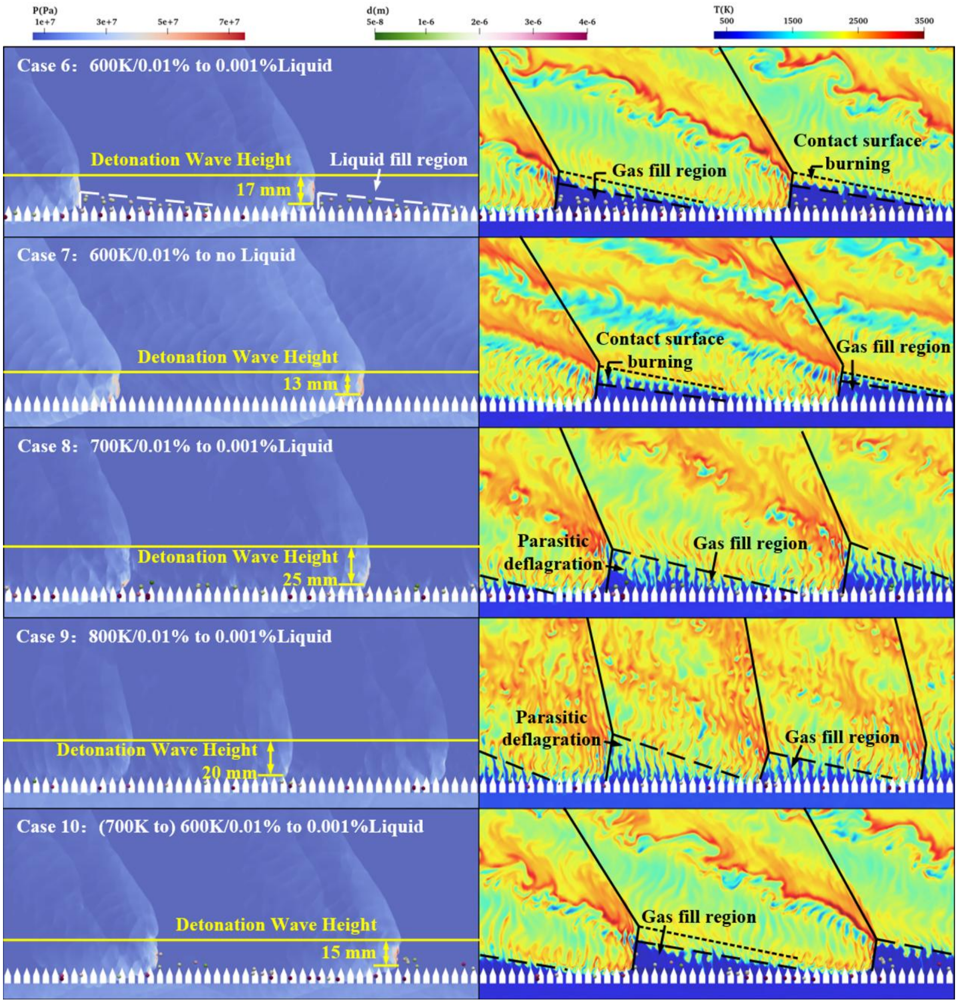

Fig 4. Instantaneous temperature and pressure for Cases 6 to 10

3.3. Combustion instability mechanism on detonation wave modes

From Sections 3.1 and 3.2, it can be observed that the incoming flow conditions for Cases 1, 4, and 5 are the same after the detonation wave stabilizes, yet the propagation modes of the detonation wave differ. These results indicate that the propagation mode of the detonation wave is not fixed with respect to the incoming flow conditions of the RDE. Rather, it is a dynamic parameter that changes with variations in the detonation flow field. Additionally, the transformation process and underlying causes are critical aspects in the study of detonation wave modes. This section provides a detailed examination of the variations in the detonation flow field as the incoming flow conditions change and analyzes the generation process and mechanism of the second detonation wave.

Figure 5 presents a schematic diagram of the droplet distribution and the position of the detonation wave in the detonation flow field under different incoming flow conditions. The size of the dots represents the size of the droplets. It can be observed that during the transition from Case 1 to Cases 2 and 3, the incoming flow temperature rises significantly, resulting in an increased vaporization rate of the droplets. Consequently, the number of droplets in the flow field decreases, while the number of detonation waves increases. In the transition from Case 1 to Case 6, the volume fraction of incoming kerosene droplets decreases, leading to a slight increase in the vaporization rate of the droplets, a further reduction in the number of droplets in the flow field, and an increase in the number of detonation waves. However, when transitioning from Case 2 to Case 8 and from Case 3 to Case 9, although the volume fraction of incoming kerosene droplets decreases, the vaporization rate of the droplets in the high-temperature flow field is already sufficiently high. Therefore, the potential increase in the vaporization rate that could result from further reducing the volume fraction of the droplets is minimal and does not significantly influence the detonation wave mode.

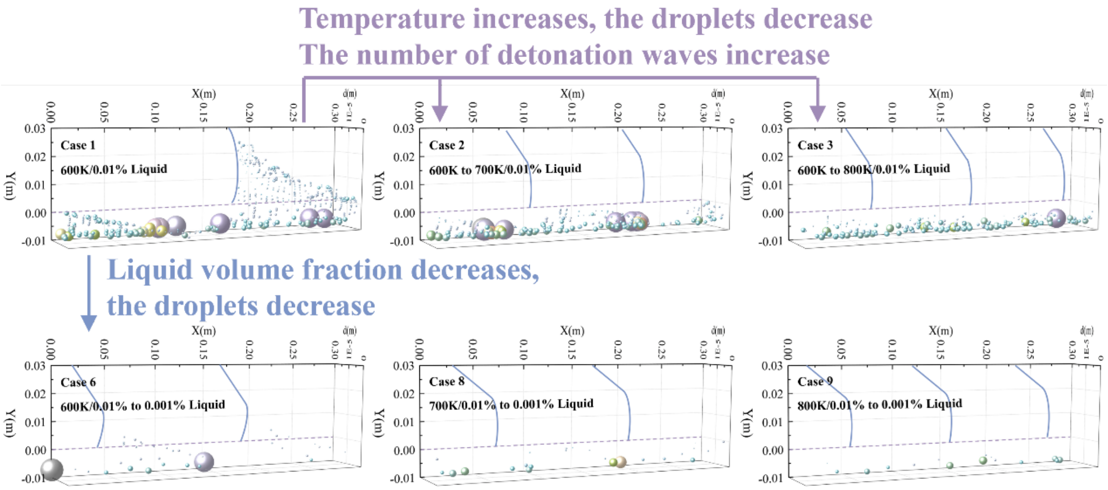

Fig 5. Schematic diagram of droplet distribution in the detonation flow field

In summary, the primary factor behind the alteration of the detonation wave mode is the high-frequency combustion instability phenomenon that arises within the rotating detonation combustor. Changes in the incoming flow conditions of the combustor, such as elevated incoming flow temperatures or a reduction in the droplet content in the fuel, can escalate the vaporization rate of droplets. The droplets may reach a critical state before complete evaporation, leading to a sudden surge in the evaporation rate. This triggers the onset of quasi-isochoric combustion processes. During this phase, the chemical reaction rate within the central control volume accelerates significantly, overshadowing the volume changes induced by local fluid motion. Consequently, all the heat released by the chemical reaction is directed towards heating the local gas, resulting in a notable surge in local pressure and the generation of pressure waves.

When the pressure wave synchronizes in phase with the heat release during the quasi-isochoric combustion process, pressure oscillations amplify through the stimulation of the chemical reaction and evaporation processes [37,38], culminating in the formation of unstable combustion due to the sustained increase in transient energy. The pressure wave progressively intensifies and undergoes a series of decoupling-re-detonation cycles until a stable detonation wave emerges, leading to a transformation in the detonation wave mode.

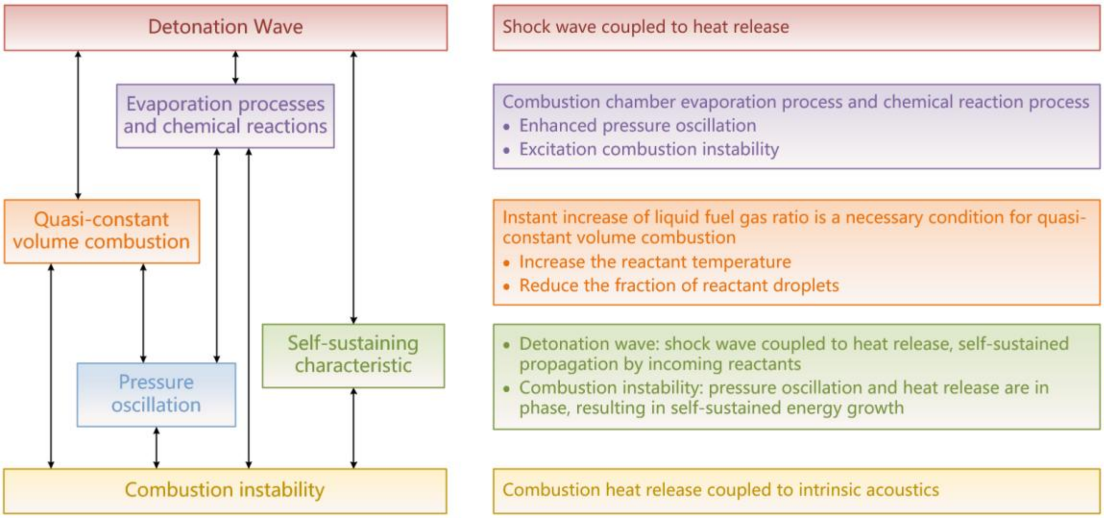

Fig 6. Correlation mechanism between detonation waves and combustion instability

4. Results and discussion

This study employs two-dimensional numerical simulation and theoretical analysis methods to investigate the evolution trend and process of the detonation wave mode within the rotating detonation combustor. The research findings are outlined as follows:

As the incoming flow temperature increases and the droplet ratio decreases, the number of detonation waves rises, with the extent of this increase depending on the range of variation in the incoming flow conditions. Additionally, when the incoming flow temperature rises, the peak pressure of the detonation wave decreases, and the parasitic combustion phenomenon ahead of the wave becomes more pronounced.

When the incoming flow temperature decreases, the number of detonation waves remains constant, and the stability of the flow field improves. A stable multi-wave mode in the rotating detonation combustor can be achieved by first increasing and then subsequently decreasing the incoming flow temperature.

In the two-phase rotating detonation combustor, the primary cause of the detonation wave mode transformation is the increase in the vaporization rate of the droplets. Both an increase in the incoming flow temperature and a decrease in the droplet proportion lead to a higher droplet vaporization rate, which subsequently induces quasi-isothermal combustion and generates pressure waves. The higher the incoming flow temperature, the sooner quasi-isovolumetric combustion occurs, resulting in a more rapid transformation of the detonation wave mode.

The process by which unstable combustion generates pressure waves that develop into detonation waves is analogous to the self-sustaining propagation of detonation waves. The disturbance in heat release caused by pressure waves leads to a self-sustaining transient increase in energy. The pressure wave undergoes multiple cycles of decoupling and re-detonation, ultimately resulting in the formation of a stable detonation wave and the final change in the detonation wave propagation mode.

References

1. Zeldovich Y B. To the question of energy use of detonation combustion[J]. Journal of propulsion and power, 2006, 22(3): 588-592.
2. Wolański P. Detonative propulsion[J]. Proceedings of the combustion Institute, 2013, 34(1): 125-158.
3. Fievisohn R T, Yu K H. Steady-state analysis of rotating detonation engine flowfields with the method of characteristics[J]. Journal of Propulsion and Power, 2017, 33(1): 89-99.
4. Kailasanath K. Review of propulsion applications of detonation waves[J]. AIAA journal, 2000, 38(9): 1698-1708.
5. Roy A, Ferguson D H, Sidwell T, et al. Experimental study of rotating detonation

combustor performance under preheat and back pressure operation[C]//55th AIAA aerospace sciences meeting. 2017: 1065.
6. Rankin B A, Richardson D R, Caswell A W, et al. Chemiluminescence imaging of an optically accessible non-premixed rotating detonation engine[J]. Combustion and Flame, 2017, 176: 12-22.
7. Wang C, Liu W, Liu S, et al. Experimental investigation on detonation combustion patterns of hydrogen/vitiated air within annular combustor[J]. Experimental Thermal and Fluid Science, 2015, 66: 269-278.
8. Fan L, Shi Q, Zhi Y, et al. Experimental and numerical study on multi-wave modes of H2/O2 rotating detonation combustor[J]. International Journal of Hydrogen Energy, 2022, 47(26): 13121-13133.
9. Bai Q, Han J, Zhang S, et al. Experimental study on the auto-initiation of rotating detonation with high-temperature hydrogen-rich gas[J]. Physics of Fluids, 2023, 35(4).
10. Bai Q, Han J, Qiu H, et al. Study on initiation characteristics of rotating detonation by auto-initiation and pre-detonation method with high-temperature hydrogen gas[J]. International Journal of Hydrogen Energy, 2024, 49: 450-461.
11. Zhai D W, Zhao N B, Jin S, et al. Numerical study on the characteristics of rotating detonation wave with multicomponent mixtures[J]. International Journal of Hydrogen Energy, 2023, 48(76): 29786-29797.
12. Frolov S M, Aksenov V S, Ivanov V S, et al. Large-scale hydrogen−air continuous detonation combustor[J]. International Journal of Hydrogen Energy, 2015, 40(3): 1616-1623.
13. Canteins G. Etude de la détonation continue rotative-Application à la propulsion[D]. Université de Poitiers, 2006.
14. Anand V, George A S, Driscoll R, et al. Longitudinal pulsed detonation instability in a rotating detonation combustor[J]. Experimental Thermal and Fluid Science, 2016, 77: 212-225.
15. Bykovskii F A, Zhdan S A, Vedernikov E F. Continuous spin detonations[J]. Journal of propulsion and power, 2006, 22(6): 1204-1216.
16. Huang X, Teo C J, Khoo B C. Wave mode dynamics in an ethylene-air rotating detonation combustor[J]. AIAA Journal, 2021, 59(5): 1808-1823.
17. Chen H, Si C, Wu Y, et al. Numerical investigation of the effect of equivalence ratio on the propagation characteristics and performance of rotating detonation engine[J]. International Journal of Hydrogen Energy, 2023, 48(62): 24074-24088.
18. Hu J, Zhang B. Time/frequency domain analysis of detonation wave propagation mechanism in a linear rotating detonation combustor[J]. Applied Thermal Engineering, 2024, 255: 124014.
19. Betelin V B, Nikitin V F, Mikhalchenko E V. 3D numerical modeling of a cylindrical RDE with an inner body extending out of the nozzle[J]. Acta Astronautica, 2020, 176: 628-646.
20. Nikitin V F, Mikhalchenko E V. Safety of a rotating detonation engine fed by acetylene–oxygen mixture launching stage[J]. Acta Astronautica, 2022, 194: 496-503.
21. Yao K, Yang P, Teng H, et al. Effects of injection parameters on propagation patterns of hydrogen-fueled rotating detonation waves[J]. international journal of hydrogen energy, 2022, 47(91): 38811-38822.
22. He X J, Liu X Y, Wang J P. On the mechanisms of the multiplicity and bifurcation of detonation waves in 3D rotating detonation engines[J]. Aerospace Science and Technology, 2022, 130: 107874.
23. Qiu H, Bai Q, Han J, et al. Effects of blockage ratio on the propagation characteristics of hydrogen-rich gas rotating detonation[J]. Physics of Fluids, 2023, 35(8).
24. Bykovskii F A, Zhdan S A, Vedernikov E F. Continuous spin detonation of hydrogen-oxygen mixtures. 1. Annular cylindrical combustors[J]. Combustion, Explosion, and Shock Waves, 2008, 44: 150-162.
25. Yi T H, Lou J, Turangan C, et al. Propulsive performance of a continuously rotating

detonation engine[J]. Journal of Propulsion and Power, 2011, 27(1): 171-181.
26. Anand V, George A S, Driscoll R, et al. Characterization of instabilities in a rotating detonation combustor[J]. International Journal of Hydrogen Energy, 2015, 40(46): 16649-16659.
27. Fotia M L, Schauer F, Kaemming T, et al. Experimental study of the performance of a rotating detonation engine with nozzle[J]. Journal of Propulsion and Power, 2016, 32(3): 674-681.
28. Yao S, Tang X, Zhang W. Adaptive operating mode switching process in rotating detonation engines[J]. Acta Astronautica, 2023, 205: 239-246.
29. Wang Y, Tian C, Yang P. Effects of ozone addition on multi-wave modes of hydrogen–air rotating detonations[J]. Aerospace, 2023, 10(5): 443.
30. Zhu Y, Wang K, Zhao M, et al. Experimental study on wave propagations in a rotating detonation chamber with different outlet configurations[J]. Acta Astronautica, 2022, 200: 388-399.
31. Kurganov A, Noelle S, Petrova G. Semidiscrete central-upwind schemes for hyperbolic conservation laws and Hamilton--Jacobi equations[J]. SIAM Journal on Scientific Computing, 2001, 23(3): 707-740.
32. Meng Q, Zhao M, Zheng H, et al. Eulerian-Lagrangian modelling of rotating detonative combustion in partially pre-vaporized n-heptane sprays with hydrogen addition[J]. Fuel, 2021, 290: 119808.
33. Zhao M, Cleary M J, Zhang H. Combustion mode and wave multiplicity in rotating detonative combustion with separate reactant injection[J]. Combustion and Flame, 2021, 225: 291-304.
34. Fan L, Shi Q, Lin W, et al. Numerical simulation of similarities between rotating detonation and high-frequency combustion instability under two mixing schemes[J]. AIP Advances, 2022, 12(2).
35. Westbrook C K, Dryer F L. Simplified reaction mechanisms for the oxidation of hydrocarbon fuels in flames[J]. Combustion science and technology, 1981, 27(1-2): 31-43.
36. Wang F, Weng C. Numerical research on two-phase kerosene/air rotating detonation engines[J]. Acta Astronautica, 2022, 192: 199-209.
37. Tong A Y, Sirignano W A. Oscillatory vaporization of fuel droplets in an unstable combustor[J]. Journal of Propulsion and Power, 1989, 5(3): 257-261.
38. Huang Y. Theoretical, numerical simulation and experimental investigations of combustion instability in liquid rocket engine [D]. National University of Defense Technology, 2001.